Langmuir

Article

pubs.acs.org/Langmuir

Swelling Enhanced Remanent Magnetization of Hydrogels Cross-Linked with Magnetic Nanoparticles

Susanne van Berkum,[†] Pieter D. Biewenga,[†] Suzanna P. Verkleij,[†] J. (Hans) B. A. van Zon,[§] Kristel W. M. Boere,[‡] Antara Pal,[†] Albert P. Philipse,[†] and Ben H. Erné*[,†]

[†]Van 't Hoff Laboratory for Physical and Colloid Chemistry, Debye Institute for Nanomaterials Science, Utrecht University, Padualaan 8, 3584 CH Utrecht, The Netherlands

[§]Philips Research Europe Laboratories, High Tech Campus 11, 5656 AE, Eindhoven, The Netherlands

[‡]Utrecht Institute for Pharmaceutical Sciences, Utrecht University, Universiteitsweg 99, 3584 CG, Utrecht, The Netherlands

Supporting Information

ABSTRACT: Hydrogels that are pH-sensitive and partially cross-linked by cobalt ferrite nanoparticles exhibit remarkable remanent magnetization behavior. The magnetic fields measured outside our thin disks of ferrogel are weak, but in the steady state, the field dependence on the magnetic content of the gels and the measurement geometry is as expected from theory. In contrast, the time-dependent behavior is surprisingly complicated. During swelling, the remanent field first rapidly increases and then slowly decreases. We ascribe the swelling-induced field enhancement to a change in the average orientation of magnetic dipolar structures, while the subsequent field drop is due to the decreasing concentration of nanoparticles. During shrinking, the field exhibits a much weaker time dependence that does not mirror the values found during swelling. These observations provide original new evidence for the markedly different spatial profiles of the pH during swelling and shrinking of hydrogels.

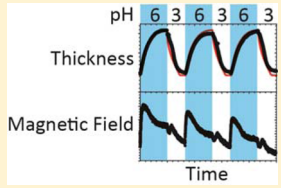

INTRODUCTION

Hydrogels are versatile materials for biomedical applications, such as drug delivery,[1−3] tissue engineering,[4] and biosensors.[5,6] An important feature of hydrogels is their responsiveness to the environment via a change in their volume. The response to external stimuli is caused by functional chemical groups, such as carboxylic acid or amide, present on the backbone of the polymer chains. Possible stimuli include changes in temperature, ionic strength, pH, and concentrations of biological molecules.[1] In the case of a gel with acidic functional groups, an increase in pH causes the gel to become charged; counterions are released inside the gel, which increases the osmotic pressure and results in swelling of the gel, to an extent that is limited by its mechanical stiffness.

In biosensor applications, an essential question is what the transducer should be: how does one detect the hydrogel volume and its changes? Optical and mechanical properties change for swelling hydrogels and provide the basis for well-investigated transducer principles.[7,8] Lee et al.[9] reported on inverse opal hydrogels, where polystyrene colloids serve as a template for a macroporous network. Boronic-acid-functionalized copolymers were incorporated in the hydrogel network to have glucose sensitivity, such that the presence of glucose induces swelling of the hydrogel and the changing periodicity causes a diffraction shift.[9] A comparable system is described by Barry et al.,[10] who used a hydrogel based on poly(acrylamide) as a humidity sensor. Environmental changes can also be detected by monitoring the mechanical properties of a hydrogel attached to a substrate. Hilt et al.[11] described a hydrogel secured on a microcantilever, where increasing pH caused bending of the microcantilever as a result of swelling of the hydrogel.

Incorporation of magnetic nanoparticles makes it possible to detect chemical changes magnetically. Song et al.[12] described a wireless sensor based on a pH-sensitive hydrogel with embedded magnetic composite microparticles; the changes in the gel's volume are detected through the shift in the self-resonant frequency of an inductive coil. This sensor type shows reversibility, reproducibility, and relatively fast detection of small changes in pH. Van Bruggen and Van Zon[13] previously proposed the theoretical concept of a sensor with a magnetic hydrogel, whose chemical changes are detected via direct measurement of the magnetic field strength; they showed that for an increasing distance between the embedded magnetic nanoparticles and the detector the strength of the magnetic field decreases. Both approaches[12,13] require a superparamagnetic hydrogel, an AC current source to magnetize the gel, and lock-in detection of the induced harmonic magnetization. We explore the feasibility of an original alternative approach: detection of the static field of a magnetically remanent hydrogel. Hydrogels with nanoparticle cross-linkers and a remanent magnetic field have been studied before,[14−19] but as far as we know, the question whether changes in the swelling degree can be detected via the remanent magnetic field has not yet been addressed. The advantage for sensors, in principle, is that this would require neither an AC current source nor lock-

Received: August 25, 2014
Revised: December 5, 2014
Published: December 8, 2014

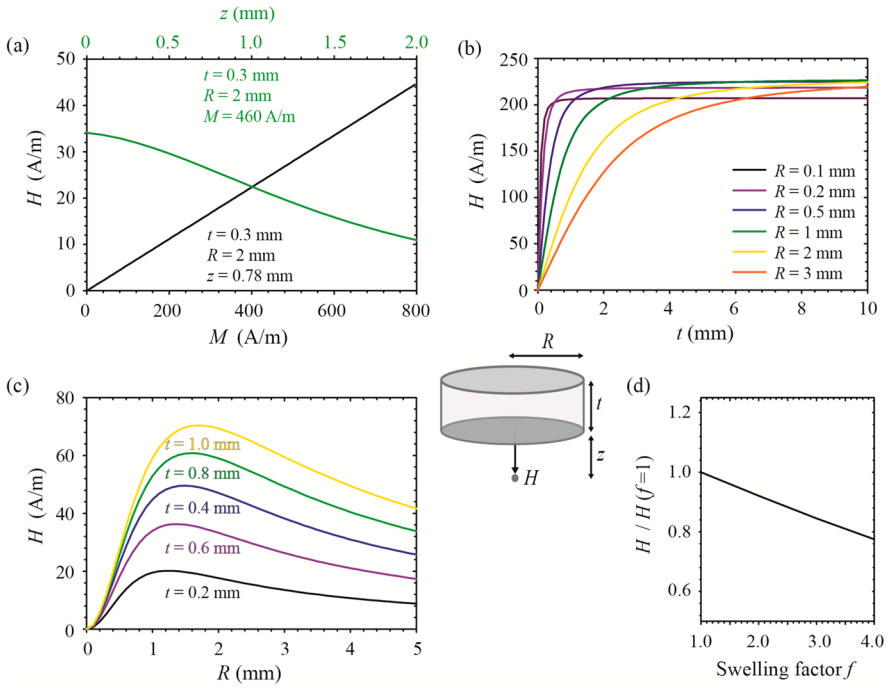

Figure 1. Calculations of the measured field H at a distance z from the bottom of a magnetized disk of radius R and thickness t (see the inset) using eqs 2 and 3. (a) Measured field H as a function of M in black and as a function of z in green. (b) Dependence on t for various values of R (z = 0.01 mm, M = 460 A/m). (c) Dependence on R for various values of t (M = 460 A/m, z = 0.78 mm). (d) Normalized measured field as a function of the swelling factor $f = t/t_0$. Here only the swelling-induced dilution effect is taken into account; see eq 3 (z = 0.78 mm, t_0 = 0.28 mm, R = 2 mm).

in detection. Here we investigate how the magnetic field depends on the measurement geometry and how it changes in time upon swelling and shrinking of the gel.

The Experimental Methods section summarizes how thin films of magnetically remanent hydrogel were prepared and how their field was measured. The Theory section focuses on the magnetic field generated by remanent ferrogels, how we expect it to depend on the measurement geometry, and how it might be affected by swelling or shrinking. The Results section presents our measurements and numerical simulations, and they are interpreted in the Discussion section.

EXPERIMENTAL METHODS

In this section, the experimental methods are briefly summarized. The chemicals, chemical synthesis recipes, and measurement procedures are described in more detail in the Supporting Information. Except when stated otherwise, experiments were at room temperature (~21 °C).

Cobalt ferrite nanoparticles with an average diameter of 22 nm and a polydispersity of 31% were prepared by coprecipitation of Co(II) and Fe(III) salts in alkaline medium and subsequently treated with nitric acid to charge them positively, as described by Tourinho et al.[20] The positive charge was important to ensure good colloidal stability of the liquid precursor mixture of the gels and irreversible chemical fixation of the nanoparticles to the polymer network.[19] Transmission electron microscopy (TEM) was performed on a Philips Tecnai 12 microscope operating at 120 kV. The nanoparticles had a dipolar contact interaction of 6 k_BT in magnitude, sufficient for the presence of small dipolar structures.[19] Further details of the synthesis of our particles are presented elsewhere.[19,21]

Thin circular layers of ferrogel were prepared by polymerization of a ferrogel mixture in a mold on a 150 μm thick glass slide. This was done without applying an external magnetic field because in external field large magnetic aggregates were formed that sedimented out of the liquid before polymerization had been completed. To ensure fixation of the thin ferrogel layers during swelling experiments, glass slides were coated with (3-trimethoxysilyl) propyl methacrylate (TPM).[22] The water-based gels were prepared from acrylic acid, hydroxylethyl acrylate, diethylene glycol diacrylate, cobalt ferrite nanoparticle dispersion, and V-50 initiator, which required heating to 80 °C to realize the polymerization. The gels contained 28 mg of nanoparticles per milliliter, corresponding to a mean distance of 100 nm between the particles. A wider glass cylinder was fixed around the ferrogel disk to serve as a container for aqueous solution of pH 3 or 6.[21]

The thickness of the ferrogel layers exposed to buffer solution was monitored using an inverted optical microscope. During swelling experiments, the field from ferrogel layers was measured using a home-built setup with a transverse Hall sensor probe with a square edge length of 1 mm.[21] Prior to a series of measurements, the gel was magnetized perpendicular to the glass slide using a square neodymium magnet; the gel was removed in the direction perpendicular to the slide to retain the orientation of the magnetic nanoparticle dipoles.

The magnetization of the ferrogels, corresponding to their internal magnetic field, was determined using an alternating gradient magnetometer. To calculate M, the remanent magnetic dipole moment of the sample was divided by the sample volume.

Small-angle X-ray scattering (SAXS) experiments were performed at the Dutch-Belgian beamline BM-26B of the European Synchrotron Radiation Facility (ESRF) in Grenoble, France using an X-ray wavelength of 1.033 Å.[23] The samples were contained in thin glass capillaries.

The frequency-dependent magnetic susceptibility of cobalt ferrite ferrofluid and ferrogel was measured in the low-field limit (170 A/m or less) using a home-built setup described by Kuipers et al.,[24] with a frequency range extended to 1 MHz using two 7280 DSP lock-in amplifiers.

Mechanical measurements on bulk gels were performed with a dynamic mechanical analyzer from TA Instruments.

THEORY

This section focuses on the magnetic field generated by remanent ferrogels. Two possible effects of swelling are examined: the magnetic field may decrease due to dilution of

dx.doi.org/10.1021/la503390w | Langmuir 2015, 31, 442−450

the gel or it may increase due to the alignment of magnetic dipolar structures.

Our later calculations of the time-dependent thickness and internal pH profiles of hydrogels are explained in the Supporting Information. For simplicity, we adopt the Donnan equilibrium theory by De et al.,[25] taking into account the diffusion of H^+ and its effects on the dissociation of hydrogel acidic groups and the resulting osmotic pressure but neglecting the effect of electric fields on the mobility of the ions. We note that our geometry differs from that of De et al.,[25] as our gels are thin films that swell mainly in the z direction.

Swelling-Induced Dilution Effect on the Magnetic Field. From the axial magnetic field of a circular current loop,[26] it follows that the axial field of an infinitesimally thin disk that is homogeneously magnetized perpendicular to it is given by

$$dH = \frac{MR^2}{2(z^2 + R^2)^{3/2}}\, dt \tag{1}$$

where dH is the field emanating from the disk, M is the magnetization (the internal magnetic field, in A/m), R is the radius, z is the distance to the center of the disk in perpendicular direction, and dt is the thickness of the disk. The axial field of a cylinder of finite thickness t at a distance z from the bottom of the cylinder is obtained replacing z by $z+t'$ in eq 1 and integrating for t' going from 0 to t

$$H = \frac{M}{2}\left[\left(\frac{z + t}{\sqrt{(z + t)^2 + R^2}}\right) - \left(\frac{z}{\sqrt{z^2 + R^2}}\right)\right] \tag{2}$$

This is the field at a point sensor, a good approximation of our experimental geometry.

When the gel swells, the concentration of nanoparticles decreases, and the field produced by the gel is expected to decrease as well. Assuming that swelling occurs only in the z direction, eq 2 leads to

$$H = \frac{M(t_0)}{2f}\left[\left(\frac{z + ft_0}{\sqrt{(z + ft_0)^2 + R^2}}\right) - \left(\frac{z}{\sqrt{z^2 + R^2}}\right)\right] \tag{3}$$

where $M(t_0)$ is the magnetization at the initial thickness of the gel, $f = t/t_0$ is the swelling factor, t is the thickness of the ferrogel, and t_0 is the initial thickness at which the gel is subjected to a magnetization treatment.

The influence of the different parameters acting in eqs 2 and 3 is examined in Figure 1. The measured field increases linearly with increasing M and decreases with increasing z (Figure 1a). For $t \ll z$, the two terms that are subtracted from each other in eq 2 are equal and H is zero, whereas for larger t, the measured magnetic field increases with increasing t, approaching a maximum value of $M/2$ (Figure 1b). As a function of R, the field shows a maximum when R is on the order of $z+t$ (Figure 1c). The swelling of a ferrogel gives an approximately linear decrease in the magnetic field with increasing swelling factor. This is illustrated in Figure 1d, where swelling by a factor of two decreases the magnetic signal by 8%.

Equation 3 will later be used to calculate the time-dependent magnetic field during swelling experiments. The ferrogel is then described by $N = 100$ horizontal slices or bins, each with the same radius R but located at its own distance z from the sensor. Moreover, each slice has its own thickness t and its own concentration of nanoparticles, depending on the local pH, resulting in a local value of the magnetization M.

Swelling-Induced Alignment of Magnetic Dipolar Structures. The magnetic contact interaction of our nanoparticles has a magnitude of 6 k_BT, sufficient for the presence of small dipolar structures.[19] Whereas the orientation of the magnetic easy axis of the nanocrystals in the hydrogel is most probably random, the z component of the nanoparticle dipoles is positive after the magnetization treatment.[27] When the gel is stretched in the z direction without changing in the other directions, elongated dipolar structures will align in the swelling direction (Figure 2a).

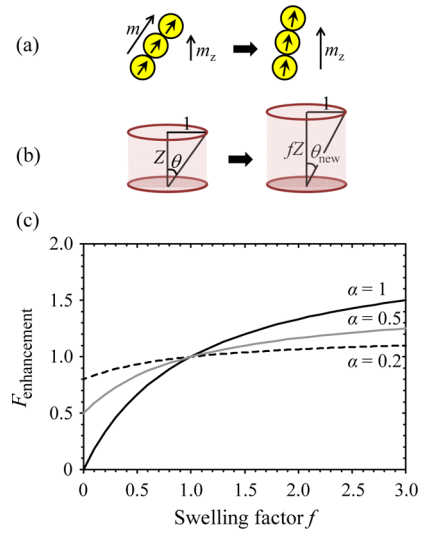

Figure 2. (a) Schematic illustration of how an elongated dipolar object that is anchored to the polymer network might be reoriented upon swelling of the gel in the z direction only. (b) Change of the angle of an orientation vector as a result of the swelling: (left) a line segment with x,z coordinates 1 and Z is at an angle θ with the z axis such that $\cot\theta = Z$ and (right) after swelling of the z component by a factor f. The angle now corresponds to $\cos\theta_{new} = fZ/(1 + (fZ)^2)^{1/2}$. (c) Field enhancement factor as a function of the swelling factor f for various values of α, the fraction of particles contributing to the swelling-induced magnetic field enhancement; see eq 9. No dilution effects of a swelling ferrogel are included in these calculations. For $f < 1$, the ferrogel shrinks.

Before swelling, each dipolar object has a magnetic moment that is at an angle θ with respect to the z axis (Figure 2b)

$$0 \le \theta \le \frac{\pi}{2} \tag{4}$$

The z component m_z is thus $m\cos\theta$, where m is the magnitude of the magnetic moment and the average remanence can be obtained by an integration of the z components over all θ and all directions in the plane perpendicular to z

$$\langle m_z\rangle = \frac{\int_0^{\pi/2} m\cos\theta\cdot 2\pi m\sin\theta\, m d\theta}{\int_0^{\pi/2} 2\pi m\sin\theta\, m d\theta} = \frac{m}{2} \tag{5}$$

In the absence of dipolar reorientation inside the nanocrystals by Néel relaxation, the magnetic remanence would thus be 50%.

Our gels swell mainly in the z direction, and consequently, elongated objects will gradually align in the z direction,

dx.doi.org/10.1021/la503390w | Langmuir 2015, 31, 442−450

resulting in an enhanced field. We will first estimate the new angle θ_{new} and then evaluate how it impacts on the remanent magnetic field.

Swelling of a ferrogel by a swelling factor f changes the z component of every point in the ferrogel by a factor f. A line segment that connects two points in the gel and that is at an angle $0 < \theta < \pi/2$ changes its orientation because the z displacement due to swelling is higher for the high-z point than for the low-z point. The new angle θ_{new} is given by (see Figure 2b)

$$\cos\theta_{new} = \frac{fZ}{\sqrt{1 + (fZ)^2}} = f\frac{\cot\theta}{\sqrt{1 + f^2\cot^2\theta}} \quad (6)$$

This expression can be inserted into eq 5 to obtain the new average z component of m, yielding

$$\langle m_z\rangle = mf\int_0^{\pi/2}\frac{\cos\theta}{\sqrt{1 + f^2\cot^2\theta}}\,d\theta \quad (7)$$

When eq 7 is divided by eq 5, an enhancement factor is found that might account for the additional alignment of nanoparticle dipoles caused by hydrogel swelling

$$F_{enhancement} = 2f\int_0^{\pi/2}\frac{\cos\theta}{\sqrt{1 + f^2\cot^2\theta}}\,d\theta = \frac{2f}{1 + f} \quad (8)$$

In eq 8, the swelling factor is by definition equal to $f = 1$ just after treatment in a saturating magnetic field, regardless of the hydration of the gel. Swelling of the gel leads to an increase in f and a corresponding increase in the alignment effect. Equation 8 assumes that all particles are part of anisometric structures that align upon swelling, but this is not likely to be the case in our experiments. To take this into account, a factor α is introduced, the effective fraction of nanoparticles that contribute to the swelling-induced alignment effect

$$F_{enhancement} = (1 - \alpha) + \alpha\frac{2f}{1 + f} \quad (9)$$

From this expression, for $\alpha = 1$, the enhancement effect is at most ~30% when the volume of the gel is doubled; see Figure 2c.

RESULTS

This section is divided into two parts. First, measurements will be presented for gels in the steady state, with characterizations of the ferrogels, magnetic signals as a function of measurement geometry, and steady-state thickness as a function of pH. Second, it will be shown how the thickness and the magnetic field of the gels change in time during swelling and shrinking.

Steady-State Measurements. The ferrohydrogels that we prepared are circular thin layers that are chemically anchored to the glass substrate and mainly swell in the z direction. Figure 3a shows schematically the typical dimensions of the gel before and after swelling. The photographs in Figures 3b,c indicate that the edge of a gel disk with a diameter of 4000 μm moves by ~400 μm when the thickness of the gel changes from 330 to 660 μm; the fixation of the gel to the substrate is imperfect, but in relative terms, the thickness expands by 100% and the width by 10%, from which we conclude that swelling is mainly in the z direction. A more dilute gel is found to be optically homogeneous (Figure 3d), but the more concentrated gels have such a dark color that inhomogeneity cannot be excluded

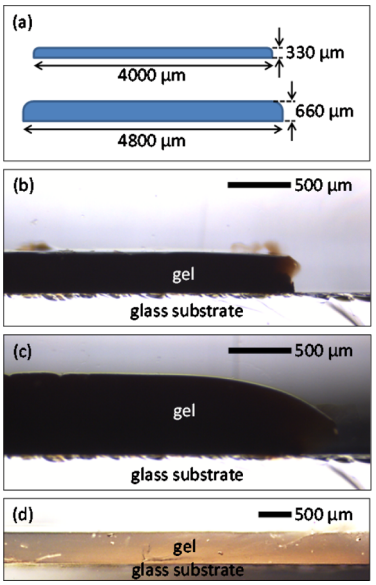

Figure 3. Cross sections of a ferrogel before and after swelling, observed by in situ optical microscopy. (a) Typical dimensions of our circular thin films before and after swelling from pH 3 to pH 6; percentually, the swelling is mainly in the z direction. (b,c) Edge of the gel (b) before and (c) after swelling. (d) Differently illuminated, wider, and more dilute gel at pH 6; it is homogeneously colored, indicating a homogeneous nanoparticle concentration. The main scratches and imperfections are reflections from the imperfectly cut side of the gel.[21]

from their appearance. We noticed no aging of the gels when they were stored for a few weeks at pH 3 or 6: the color, solidity, and magnetic properties remained the same. At pH 2, however, the magnetic remanence decreased about twice more rapidly than could be ascribed to Néel relaxation, and this was due to slow chemical dissolution of the cobalt ferrite.

The ferrohydrogels contain cobalt ferrite nanocrystals, as imaged by TEM in Figure 4a. The particles are highly polydisperse (22 nm average diameter, 31% polydispersity) and show a tendency to self-assemble into strands. The 2D SAXS scattering patterns in the insets of Figure 4b are radially symmetric, indicating that before swelling, the nanoparticle structures are isotropically distributed in the gel. In preliminary experiments, we attempted to synthesize gels in an external magnetic field, which yielded strongly anisotropic scattering, but the particles had largely sedimented to the bottom of the sample before polymerization was complete. Unfortunately, we were not able to use SAXS to characterize the effects of swelling on sample structure in situ. Moreover, no Bragg peak is present in the scattering patterns in Figure 4b, which would have allowed a more quantitative analysis. Nevertheless, the scaling of the scattered intensity on the wave vector q contains important information on the morphology and size of the structures.

At low q, the SAXS intensity scales with $q^{-1.55}$; at high q it scales with $q^{-3.55}$; and the transition between the two regimes occurs at $2\pi/q$ on the order of 30 nm. The scaling informs about the morphology of the scattering objects, with exponents −1, −2, −3, and −4 corresponding, respectively, to 1-D rods, 2-D flat objects, 3-D fractal objects, and locally probed abrupt interfaces.[28] The $q^{-1.55}$ power law dependence at low q therefore indicates that, on larger length scales than 30 nm, the structure is in-between straight linear objects and flat plates, which agrees with the presence of semiflexible chains of

dx.doi.org/10.1021/la503390w | Langmuir 2015, 31, 442−450

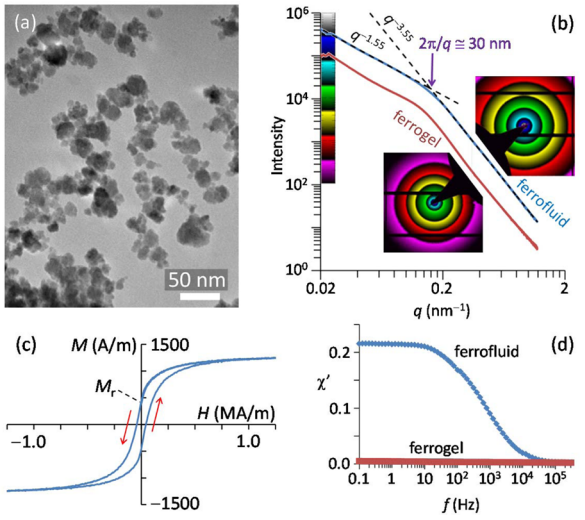

Figure 4. Characterizations of ferrogel microstructure: (a) TEM micrograph of the cobalt ferrite nanoparticles, (b) X-ray scattering intensity versus wave vector q for the same cobalt ferrite particles in liquid and in gel (the insets are the scattering patterns), (c) magnetization of ferrogel versus external magnetic field, and (d) frequency dependence of the in-phase component of the magnetic susceptibility at the same concentration of nanoparticles in liquid and gel.[19]

nanoparticles. The $q^{-3.55}$ power law dependence at high q indicates the presence of sharp interfaces on length scales below 30 nm, which we ascribe to scattering at the surface of the nanoparticles. The value of π/q or $2\pi/q$ at the transition between the two regimes gives an estimate of object size,[28] here about 15 to 30 nm, in agreement with the TEM size of the nanocrystals. The scaling of the scattered intensity on the wave vector q is practically the same when the nanoparticles are in the gel and when they are dispersed in a liquid, suggesting that the nanoparticle structures are similar.

The steady-state magnetization of the ferrogels was characterized in two ways. A typical magnetization curve is shown in Figure 4c, indicating a remanence of 37%. Figure 4d presents the real components of two magnetic susceptibility spectra for the same concentration of particles in a liquid and in a ferrogel.[19] Upon confinement in a hydrogel, the magnetic nanoparticles are no longer able to move, as expected from the chemical coupling of the particles to the hydrogel network.[19]

Figure 5 shows how the external field H of ferrogel disks depends on magnetic content and measurement geometry. Changes in the nanoparticle concentration cause the field to increase linearly with the magnetization M (Figure 5a). At constant particle concentration and therefore also constant M, the field decreases as the distance z from gel to sensor increases (Figure 5b), the field increases with gel thickness t (Figure 5c), and a maximum is found when the radius R is on the order of $z + t$ (Figure 5d). These experimental results are in fairly good quantitative agreement with theory, so that we can use eq 2 later in our discussion of swelling-dependent changes of the magnetic field.

Figure 6 shows the equilibrium thickness of our ferrogels as a function of pH. The fit[21] indicates an effective pK_a of 4.7, close to 4.5 that we obtained for hydrogels prepared in the same way except without nanoparticles. The pH response was slightly greater than without nanoparticles. We speculate that the nanoparticles act as nuclei during the polymerization process,

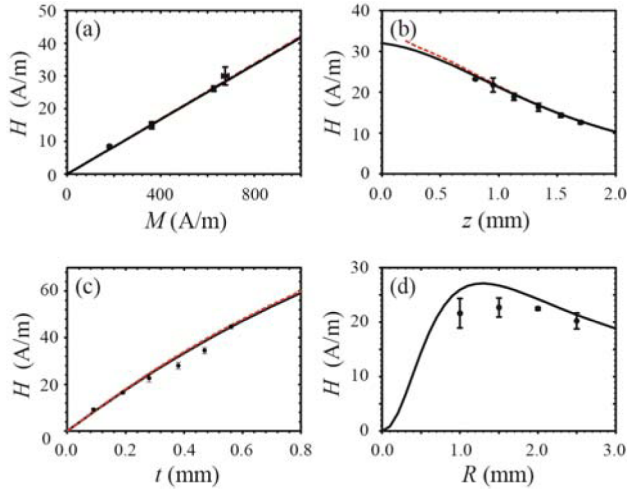

Figure 5. Experimental verification of eq 2: dependence of the measured field H as a function of (a) M, (b) z, (c) t, and (d) R (see inset of Figure 1). Default values of the experimental parameters were R = 2 mm, t = 0.28 mm, z = 0.78 mm, and M = 460 A/m.

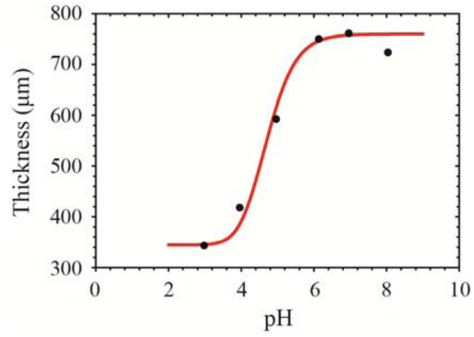

Figure 6. Equilibrium thickness of a ferrogel layer as a function of pH, with a theoretical calculation indicated by the red line.[21]

promoting an increased polymer concentration in their direct vicinity and a lower polymer density in between nanoparticle assemblies, softening the gel. On the basis of gel volume and concentration of ionizable groups, we estimate a Young's modulus on the order of 320 Pa.[21] Measurements of the Young's modulus by dynamic mechanical analysis (DMA) confirm that despite having a similar molecular composition, the ferrogels are softer than without nanoparticles. The Young's modulus from DMA was on the order of 5 kPa, roughly 30% lower than without nanoparticles. More quantitative DMA results are not reported here because our relatively soft gels underwent an initial compression of ~25% before the force ramp could be started. As a result, the gels were much more dense than before a mechanical force was applied, yielding an overestimate of the Young's modulus.

Dynamic Measurements. Figure 7 shows three consecutive swelling and shrinking cycles of a ferrogel layer. After each full cycle, the original thickness is recovered, indicating that the processes are reversible (Figure 7a). Whereas, at least qualitatively, the time-dependent evolution of gel thickness is as expected from theory,[25] the changes in the magnetic field are surprising. Upon swelling, the magnetic field initially does not decrease but it increases (Figures 7b and 7c). This occurs in a similar, although not exactly identical, way when the initial magnetization treatment of the ferrogel is performed in the swollen or in the shrunken state. The fact that the field

dx.doi.org/10.1021/la503390w | Langmuir 2015, 31, 442−450

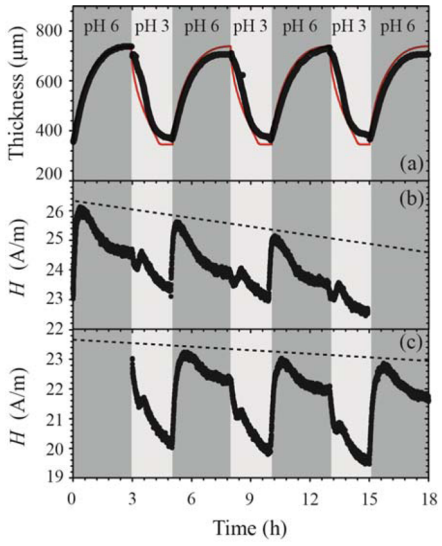

Figure 7. Three consecutive swelling and shrinking cycles on the same thin ferrogel layer in external solutions of pH 6 and pH 3. (a) Thickness of the ferrogel layer and (b,c) remanent magnetic field after saturation magnetization treatment (b) in the shrunken state at pH 3 and (c) in the swollen state at pH 6. In panel a, the red curve shows the result of numerical simulations.[25] In panels b and c, the dotted lines indicate slow decrease due to Néel relaxation of magnetic dipoles inside nanocrystals too small to produce longer term remanence.

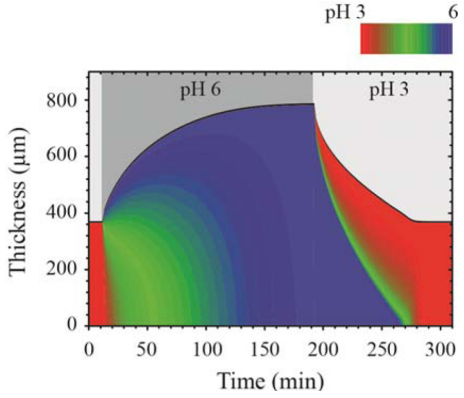

Figure 8. Calculated pH profiles in a hydrogel during swelling at pH 6 and shrinking at pH 3.[21] During swelling, the pH changes gradually across the entire gel, whereas during shrinking, there is a narrow zone with a high pH gradient moving into the gel until it is fully shrunken.

increases upon swelling is in sharp contrast with the predictions from eq 3 that take into account the decreasing concentration of magnetic nanoparticles. The observed magnetic changes are reproducible for each swelling event as well as for each shrinking event. However, the changes upon swelling are not mirrored by those upon shrinking. As soon as the swelling starts, the magnetic field first increases sharply. After ~15 min, a maximum field is reached, after which the field decreases until the ferrogel layer is swollen to equilibrium. Despite the final decrease, the field is then still higher than before swelling, although the difference is small: in the second cycle of Figure 7b, the remanent field is 23.5 A/m before swelling and 24 A/m after completion of the swelling processes, only ~2% higher. Further swelling to higher pH leads to a field that is even lower than before swelling.[21] The shrinking curve does not reproduce the same strong maximum found during swelling. The field now mainly decreases, until equilibrium thickness is reached again.

To account for the strikingly different time dependence of the magnetic field upon swelling and shrinking, let us first consider the theoretically expected pH profiles upon swelling and shrinking (Figure 8). During swelling, the pH changes relatively gradually throughout the gel. During shrinking, however, a narrow region is formed with a high pH gradient: from the moment when the ferrogel is exposed to buffer solution of lower pH, H^+ ions diffuse into the gel, bind to the deprotonated acid groups, and the ferrogel shrinks only locally. As H^+ ions diffuse further into the hydrogel, they quickly bind to deprotonated groups, and the region where pH changes remains narrow. The weaker pH gradients during swelling compared to shrinking are a well-known effect, and this explains why hydrogels swell more slowly than that they shrink.[25]

We argue that the strongly different pH profiles upon swelling and shrinking are at the origin of the very different time dependences of the magnetic field. Magnetic particles at a particular position in the gel give their own contribution to the field that is measured at the sensor, and this contribution may change in two ways: (1) as the gel swells, the distance from the particles to the sensor increases, which will tend to decrease the measured field, and (2) the swelling may help to align magnetic dipolar structures in the swelling direction, which will tend to increase the measured field. Figure 9 illustrates schematically

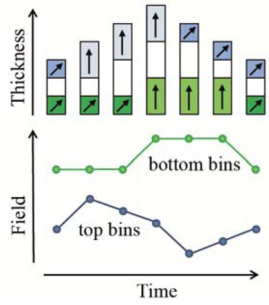

Figure 9. Schematic illustration of the time-dependent magnetic field below a remanent ferrogel during swelling and shrinking: (top) the arrows that point up represent parts of the gel where the magnetic dipolar structures are aligned in the swelling direction, whereas this is not yet the case where the arrows are slanted; (bottom) contributions from the top and bottom parts of the gel to the magnetic field measured below the gel.

how this can lead to complicated time dependence of the magnetic field measured outside the gel. Swelling starts in the top part of the gel, which contacts the external solution, causing an abrupt initial increase in the measured field. Further swelling increases the distance from the top part of the gel to the sensor, leading to a decreased contribution to the measured field. The inner parts of the gel start to swell or to shrink later, leading to a delayed change in their contributions to the magnetic field.

Further illustration of our explanation of the time-dependent magnetic field is given in Figure 10. The behavior that we had expected before starting our experiments is shown in Figure 10b with $\alpha = 0$: the field decreases upon swelling of the gel and increases upon shrinking. The swelling-induced increase in the magnetic field that we actually measured is accounted for by the alignment of magnetic dipolar structures to an extent described by a parameter α (eq 9). In our numerical simulations,[25] the gel consists of 100 bins, so that each bin initially represents 1% of

dx.doi.org/10.1021/la503390w | Langmuir 2015, 31, 442−450

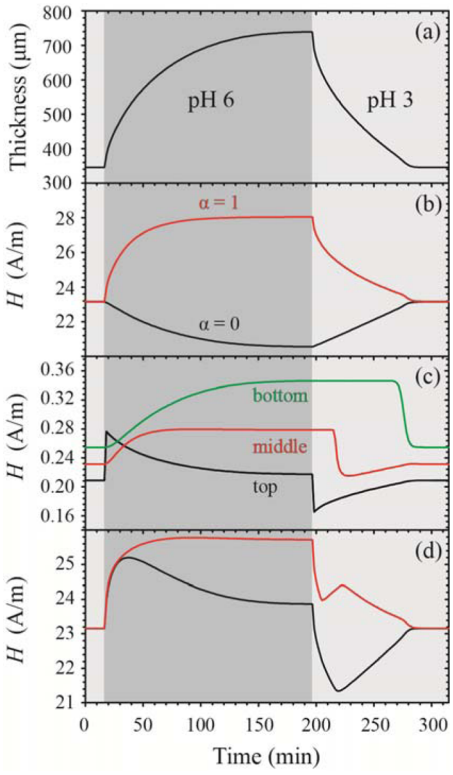

Figure 10. Simulations of (a) thickness and (b–d) magnetic field from a film of remanent ferrogel during a swelling–shrinking cycle:[21] (b) initially homogeneous concentration of magnetic material and α =1 or α = 0 (eq 9); (c) contributions from three different locations (single bins) in a gel with α = 1; and (d) bottom curve (in black) for an initially homogeneous concentration of magnetic material but α =1 in the upper half of the gel and α = 0 in the lower half and top curve (in red) for a more complicated profile in bottom bins 0–44 an initial field of M = 375 A/m and α = 0.8, in bins 45–69 M = 275 A/m and α = 0.0, in bins 70–84 M = 415 A/m and α = 0.9, and in bins 85–99 M = 440 A/m and α = 1.0.

the gel's thickness. As shown in Figure 10c, the top bin is farthest away from the field sensor and therefore initially results in the smallest field. As expected, a change in pH first affects the top bin before affecting the inner bins. The precise profiles of the concentration of magnetic material and degree of dipolar structure formation determine the time-dependent magnetic field. The upper curve in Figure 10d resembles the experiments in Figure 7c, while the lower curve in Figure 10d better reproduces the initial swelling behavior in Figure 7b. These simulations do not reproduce the experiments quantitatively, but essential aspects are recovered. Swelling causes the field first to increase and then to decrease; the shrinking starts with a sudden drop of the field and differs strongly from the curve that would be obtained by retracing the swelling curve in the inverse time direction; and the changes are on the order of 10% of the total measured field.

DISCUSSION

Our experimental results demonstrate that the field from a magnetically remanent hydrogel changes reproducibly upon swelling or shrinking. The remanent fields that we measure are very weak, in agreement with theory. However, the time-dependent behavior is unexpectedly complicated, for which we provide a qualitative explanation.

In the steady state, the weak fields of our remanent ferrogels are well accounted for by theory. In our experiments, the field inside the ferrogels was about 10 times the earth magnetic field, while the measured fields were only about half the earth magnetic field. In principle, to increase the measured signals beyond what we achieved, one might increase the concentration of magnetic nanoparticles. However, this will make it more difficult to prevent nanoparticle aggregation and inhomogeneous polymerization during chemical synthesis of the gel. Measurement geometry is another key factor determining the measured field. Theoretically, the maximum field that might be detected is half the internal field of the gel, but in practice, this limiting case seems difficult to achieve. The gel film would more or less have to touch the sensor, have a width comparable to the sensor, and be much thicker than it is wide. The fairly good quantitative agreement of the measurements with the presented theory implies that such theory could be used to optimize the measurement geometry to obtain stronger signals.

The time-dependent magnetization of our ferrogels is more complicated than expected. Upon swelling of the gel, the field first increases, whereas further swelling causes the field to decrease as the gel becomes more dilute. If the gels swell even more, the field comes back to the initial value in the shrunken state or becomes even lower;[21] this illustrates why the swelling-induced enhancement effect is a problem for the proposed biosensor application. The only way to account for the initial field enhancement during swelling seems to be an increased magnetic alignment due to a change in the orientation of remanent magnetic dipolar structures. Our cobalt ferrite nanoparticles are polydisperse and partially large enough for magnetic aggregation into clusters of a few particles. In theory, one way to avoid the swelling-dependent alignment effect would be to prealign the magnetic structures by preparing the hydrogels in a homogeneous magnetic field. However, in preliminary experiments we found that an external field creates very large magnetic self-assembly structures that sediment rapidly during preparation of the gel, as expected from cryogenic electron microscopy on ferrofluids.[29] Another approach would be to avoid the formation of dipolar structures altogether. The particles would then have to be sufficiently large to ensure slow Néel relaxation, but at the same time they would have to be provided with a sufficiently thick non-magnetic shell to keep the particles from aggregating by magnetic interactions during the preparation of the gel. The contact interaction should be weaker than a few times the thermal energy k_BT.[30]

Our numerical model accounts for main aspects of the time-dependent magnetization of our gels, but the experimental data are not reproduced quantitatively. It is useful to examine the simplifications that we made. First, our mathematical description of the swelling-induced enhancement of the magnetization (eqs 8 and 9) neglects any changes that may occur in the magnetic dipolar structures other than their orientation. Second, the experimental concentration of nanoparticles is probably not homogeneous in the freshly synthesized ferrogels. The polymerization reaction is likely to proceed at different rates at the substrate and in the interior of the gel, where heat from the exothermic reaction is less well dissipated. As a result, during chemical synthesis, the temporary degree of polymerization will depend on the position in the gel, and nanoparticles can be pushed out toward zones where polymerization has not yet progressed as far. Third, our

dx.doi.org/10.1021/la503390w | Langmuir 2015, 31, 442–450

description of the swelling process is oversimplified. The mobility of H^+ in the hydrogel is taken constant, but in practice, it is likely to depend on the local degree of dissociation of the acidic groups. From experimental work on membranes, it is clear that the diffusion of ions through charged nanoporous networks is much slower than when the networks are uncharged,[31] which in our case would depend on the local pH. Moreover, our calculations neglect the effect of local gradients of the electrical potential on the mobility of the ions, an assumption that is probably better during swelling than during shrinking, when the electric fields are higher.[25] A more detailed model with more parameters would no doubt give a better fit of our data, but our present model already succeeds in capturing the essence of the observed behavior.

CONCLUSIONS

In conclusion, the magnetic fields of our remanent ferrogels are understood quantitatively in the steady state and qualitatively as a function of time. With respect to applications in biosensors, the currently measured fields are too weak to provide an advantage over a high-frequency approach that benefits from the enhanced sensitivity of lock-in detection. Nevertheless, the time dependence of the measured field is remarkable. The key to understand it is the evolution of the spatial pH profile, which determines the local orientations of magnetic dipolar structures and their distances from the field detector. As a result, when the gel is far from equilibrium, the magnetic field at a particular thickness is different during swelling and shrinking. In a certain sense, the remanent magnetic structures act as local probes of the degree of swelling, giving a new insight into the spatial dependence of the changes that occur inside the gel.

ASSOCIATED CONTENT

Supporting Information

Experimental details of the chemical preparations and measurements, time-dependent evolution of magnetic remanence upon swelling from pH 3 to different higher pH values, hydrogel swelling theory, and numerical simulations approach. This material is available free of charge via the Internet at http://pubs.acs.org.

AUTHOR INFORMATION

Corresponding Author

*E-mail: b.h.erne@uu.nl.

Notes

The authors declare no competing financial interest.

ACKNOWLEDGMENTS

We thank Bonny Kuipers for designing and Emile Bakelaar for interfacing the magnetic remanence setup, Mark Vis for help with Mathematica, Tina Vermonden and Wim Hennink for enabling the DMA measurements, and Michel van Bruggen, Hans Tromp, Bennie ten Haken, Eduardo Mendes, and Andrei Petukhov for helpful discussions. A. Pal thanks The Netherlands Organization for Scientific Research (NWO) (700.10.355). This research is supported by the Dutch Technology Foundation STW, which is part of The Netherlands Organisation for Scientific Research (NWO) and which is partially funded by the Ministry of Economic Affairs.

REFERENCES

(1) Gupta, P.; Vermani, K.; Garg, S. Hydrogels: From Controlled Release to pH-Responsive Drug Delivery. *Drug Discovery Today* **2002**, *7*, 569−579.
(2) Qin, J.; Asempah, I.; Laurent, S.; Fornara, A.; Muller, R. N.; Muhammed, M. Injectable Superparamagnetic Ferrogels for Controlled Release of Hydrophobic Drugs. *Adv. Mater.* **2009**, *21*, 1354−1357.
(3) Pankhurst, Q.; Connolly, J.; Jones, S.; Dobson, J. Applications of Magnetic Nanoparticles in Biomedicine. *J. Phys. D* **2003**, *36*, R167−R181.
(4) Lee, K.; Mooney, D. Hydrogels for Tissue Engineering. *Chem. Rev.* **2001**, *101*, 1869−1879.
(5) Urban, G. A.; Weiss, T. Hydrogels for Biosensors. *Springer Ser. Chem. Sens. Biosens.* **2010**, *6*, 197−220.
(6) Han, I.; Han, M.; Kim, J.; Lew, S.; Lee, Y.; Horkay, F.; Magda, J. Constant-Volume Hydrogel Osmometer: A New Device Concept for Miniature Biosensors. *Biomacromolecules* **2002**, *3*, 1271−1275.
(7) Holtz, J.; Asher, S. Polymerized Colloidal Crystal Hydrogel Films as Intelligent Chemical Sensing Materials. *Nature* **1997**, *389*, 829−832.
(8) Richter, A.; Paschew, G.; Klatt, S.; Lienig, J.; Arndt, K. F.; Adler, H. J. P. Review on Hydrogel-Based pH Sensors and Microsensors. *Sensors* **2008**, *8*, 561−581.
(9) Lee, Y.; Pruzinsky, S.; Braun, P. Glucose-Sensitive Inverse Opal Hydrogels: Analysis of Optical Diffraction Response. *Langmuir* **2004**, *20*, 3096−3106.
(10) Barry, R.; Wiltzius, P. Humidity-Sensing Inverse Opal Hydrogels. *Langmuir* **2006**, *22*, 1369−1374.
(11) Hilt, J.; Gupta, A.; Bashir, R.; Peppas, N. Ultrasensitive Biomems Sensors Based on Microcantilevers Patterned with Environmentally Responsive Hydrogels. *Biomed. Microdevices* **2003**, *5*, 177−184.
(12) Song, S. H.; Park, J. H.; Chitnis, G.; Siegel, R. A.; Ziaie, B. A Wireless Chemical Sensor Featuring Iron Oxide Nanoparticle-Embedded Hydrogels. *Sens. Actuators, B* **2014**, *193*, 925−930.
(13) van Bruggen, M. P. B.; van Zon, J. B. A. Theoretical Description of a Responsive Magneto-Hydrogel Transduction Principle. *Sens. Actuators, A* **2010**, *158*, 240−248.
(14) Bonini, M.; Lenz, S.; Giorgi, R.; Baglioni, P. Nanomagnetic Sponges for the Cleaning of Works of Art. *Langmuir* **2007**, *23*, 8681−8685.
(15) Messing, R.; Frickel, N.; Belkoura, L.; Strey, R.; Rahn, H.; Odenbach, S.; Schmidt, A.M. Cobalt Ferrite Nanoparticles as Multifunctional Cross-Linkers in PAAm Ferrohydrogels. *Macromolecules* **2011**, *44*, 2990−2999.
(16) Frickel, N.; Messing, R.; Schmidt, A. M. Magneto-Mechanical Coupling in $CoFe_2O_4$-linked PAAm Ferrohydrogels. *J. Mater. Chem.* **2011**, *21*, 8466−8474.
(17) Barbucci, R.; Pasqui, D.; Giani, G.; De Cagna, M.; Fini, M.; Giardino, R.; Atrei, A. A Novel Strategy for Engineering Hydrogels with Ferromagnetic Nanoparticles as Crosslinkers of the Polymer Chains. Potential Applications as a Targeted Drug Delivery System. *Soft Matter* **2011**, *7*, 5558−5565.
(18) Ilg, P. Stimuli-Responsive Hydrogels Cross-Linked by Magnetic Nanoparticles. *Soft Matter* **2013**, *9*, 3465−3468.
(19) van Berkum, S.; Dee, J. T.; Philipse, A. P.; Erne, B. H. Frequency-Dependent Magnetic Susceptibility of Magnetite and Cobalt Ferrite Nanoparticles Embedded in PAA Hydrogel. *Int. J. Mol. Sci.* **2013**, *14*, 10162−10177.
(20) Tourinho, F.; Franck, R.; Massart, R. Aqueous Ferrofluids Based on Manganese and Cobalt Ferrites. *J. Mater. Sci.* **1990**, *25*, 3249−3254.
(21) See the Supporting Information.
(22) Hjerten, S. High-Performance Electrophoresis - Elimination of Electroendosmosis and Solute Adsorption. *J. Chromatogr.* **1985**, *347*, 191−198.
(23) Borsboom, M.; Bras, W.; Cerjak, I.; Detollenaere, D.; van Loon, D. G.; Goedtkindt, P.; Konijnenburg, M.; Lassing, P.; Levine, Y. K.; Munneke, B.; Oversluizen, M.; van Tol, R.; Vlieg, E. The Dutch-

Belgian Beamline at the ESRF. *J. Synchrotron Radiat.* **1998**, *5*, 518−520.
(24) Kuipers, B. W. M.; Bakelaar, I. A.; Klokkenburg, M.; Erné, B. H. Complex Magnetic Susceptibility Setup for Spectroscopy in the Extremely Low-Frequency Range. *Rev. Sci. Instrum.* **2008**, *79*, 013901.
(25) De, S.; Aluru, N. A Chemo-Electro-Mechanical Mathematical Model for Simulation of pH Sensitive Hydrogels. *Mech. Mater.* **2004**, *36*, 395−410.
(26) Young, H. D.; Freedman, R. A. *University Physics*; Pearson Education, Inc.: San Francisco, 2004; p 1077.
(27) van Berkum, S.; Erné, B. H. Demagnetization Treatment of Remanent Composite Microspheres Studied by Alternating Current Susceptibility Measurements. *Int. J. Mol. Sci.* **2013**, *14*, 18093−18109.
(28) Huggins, J. S.; Benoit, H. C. *Form Factors, Polymers and Neutron Scattering*; Oxford University Press, Inc.; New York, 1994; pp 165−174.
(29) Klokkenburg, M.; Erne, B. H.; Meeldijk, J. D.; Wiedenmann, A.; Petukhov, A.V.; Dullens, R. P. A.; Philipse, A.P. In situ Imaging of Field-Induced Hexagonal Columns in Magnetite Ferrofluids. *Phys. Rev. Lett.* **2006**, *97*, 185702.
(30) Klokkenburg, M.; Dullens, R.; Kegel, W.; Erne, B.; Philipse, A. Quantitative Real-Space Analysis of Self-Assembled Structures of Magnetic Dipolar Colloids. *Phys. Rev. Lett.* **2006**, *96*, 037203.
(31) Romero, V.; Vazquez, M. I.; Benavente, J. Study of Ionic and Diffusive Transport through a Regenerated Cellulose Nanoporous Membrane. *J. Membr. Sci.* **2013**, *433*, 152−159.